Research Article

Łukasz Kaczmarek*, Paweł Dobak, Tomasz Szczepański, and Kamil Kiełbasiński

Triaxial creep tests of glacitectonically disturbed stiff clay – structural, strength, and slope stability aspects

https://doi.org/10.1515/geo-2020-0291
received March 22, 2021; accepted July 28, 2021

Abstract: This study concerns the creep impact on strength parameters of the selected very cohesive soils (PI = 30–70%). The analysis refers to Neogene clays characterized by a complex structure, resulting directly from a complicated load history in the geological time scale and identified glacitectonic deformations. In the process of samples' preparation for strength tests as well as during the interpretation of the post-failure state, particular attention was paid to the soil structure. The imaging methods (X-ray densitometry and computer microtomography) enabled the comparison of the soil structure and the selection of samples with similar characteristics. The completed program of strength tests consisted of two series of tests in the triaxial stress state, differentiated by the occurrence of the initial creep stage, preceding the typical strength test scheme under undrained conditions. This study allowed to obtain a quantitative assessment of the influence of the creep process on the strength parameters of tested soils. Constant stress lower than 60% of the shear stress deviator leads to the deceleration creep course (m parameter 0.64–0.89). As a result, higher values of internal friction angle (20% increase comparing to triaxial tests without creep stage) and cohesion reduction are obtained from triaxial creep tests. Creep parameter m is found to be a valuable indicator for differentiation of landslide activity trend. The tests proved low values of axial strains (1–5%) at failure, which was associated with lithogenesis. By the implementation of obtained strength parameters into the 3D finite element model of the slope, the potential influence of the creep process on the stability of an exemplary cross section of the Warsaw slope could be determined.

Keywords: Neogene clay, strength, X-ray computed microtomography, Warsaw slope, undrained triaxial test, safety factor

1 Introduction

The diversity of the strength parameters of the soil depends on many factors, among which structural features are particularly significant. They result from the genesis and post-sedimentation transformations of sediments, which have been determined by complex, sometimes multi-stage geological history. The transformation of soil strength is influenced by changes in geostatic stresses, pre-consolidation, glacitectonics, and also – at shallow depths – disintegration caused by weathering [1–4].

The soil genesis affects the course of geodynamic processes within the slopes. Both large-scale shears due to sudden landslide movements as well as slow creep are considered in the slope stability analysis, whereas the second factor is less frequently analyzed. The creep process is considered as a displacement of soil materials along the slope with different speeds and intensities. The character of creep refers both to slow displacements of quasi-stiff parts of soil materials and the internal deformations of the soil caused by the constant or variable non-failure load.

Various aspects of the creep mechanisms can be found in numerous articles [5–9]. Based on these publications, it can be concluded that the creep process is related to the transformation of the structure and its adjustment to changes of forces occurring within the slope in the equilibrium state. The deformation of the structure is induced by the failure of bonds in a microstructural scale, the interaction of clay minerals, water absorbed on the surface of the particles, displacements of the liquid phase, and the structural viscosity of the soil.

* **Corresponding author: Łukasz Kaczmarek,** Faculty of Building Services, Hydro and Environmental Engineering, Warsaw University of Technology, Nowowiejska 20 St., 00-653 Warsaw, Poland, e-mail: lukasz.kaczmarek@pw.edu.pl
Paweł Dobak, Tomasz Szczepański, Kamil Kiełbasiński: Faculty of Geology, University of Warsaw, Żwirki i Wigury 93 St., 02-089 Warsaw, Poland

The comprehensive prediction of creep displacements is not possible only on the basis of microscale mechanisms [6]. In geological and engineering issues, the genesis diversity of soils should also be taken into consideration. Hence, in determining the rheological properties of a specific soil layer, the response of the soil to various factors of physical and mechanical characteristics as well as those related to changes in the spatial management is taken into account.

The slopes of the post-glacial upland located in the urban area of Warsaw falling toward the Vistula River valley are an interesting example of heterogeneous geodynamic behavior. As a result of the anthropogenic activity of the sloping relief and the successive loading by constructions, slow displacements with variable dynamics are observed [10]. They were conditioned both by the creeping of Quaternary and anthropogenic surface formations as well as by deeper geodynamic response resulting from the variable inclination of the roof of the underlying, glacitectonically disturbed, Neogene (Mio-Pliocene) hollow formation known as spotted clays. In this study, the relationship of structural features and creep toward shear strength was analyzed, taking into consideration these clays collected from the area of the Warsaw slope.

In the study of creep, particular attention was paid to microcracks present in tested soil and their spatial arrangement visible at various scales. These features maybe an important reason for explaining the mechanism of transformations of the investigated soil in the past and currently influencing changes in soil strength. In the research program, non-invasive and non-destructive methods of imaging the heterogeneity of the structure were used, and two methods were applied: microtomography and densitometry. They allowed to obtain the characteristics of tested material and to observe the influence of changes in laboratory loading programs. The parameters of creep and shear strength obtained from laboratory tests were used in numerical modeling of the equilibrium state of slopes and glacitectonically disturbed substrate.

2 Geological conditions of spotted clays formation in the vicinity of the Warsaw slope

In this study, samples were taken from the upland part of Warsaw in the city center. Additionally, the spotted clays sampled at the bottom of the Vistula River valley (Powiśle district) were also included in the research but as they do not correspond to the main purpose of the analysis of the creep effect on strength parameters, which will not be discussed in more detail in this study. The choice of this type of soil resulted from its complex geological history and the diversified geodynamic behavior reported for this area [11].

The analyzed formation of Neogene spotted clays was deposited in a large, hollow reservoir, covering central Poland [12]. During the subsequent several quaternary glaciations, these formations were significantly deformed by glacitectonical processes [13]. Numerous elevations and lowerings of the clay formation roof have been documented in Warsaw [14]. Spatial variability of spotted clays arrangement was caused not only by glacitectonics but also by later fluvioglacial activity and multidirectional river erosion.

In the direct vicinity of the Warsaw slope, there is a linear, elevated structure in SSE-NNW direction consisting of a number of elevations, including Mokotow, City Centre, Wawrzyszew, and Burakow (the names refer to the districts of Warsaw). The character of the spatial differentiation of the Mio-Pliocene clays roof is shown in Figure 1.

More detailed research on geological, engineering, and geotechnical conditions of Mio-Pliocene clays (e.g. refs [15,16]) showed significant diversity of the clay roof even at small distances. For example, on Piękna Street (several dozen meters north from the test site of this study), two extremely different lithological profiles were documented (Figure 2) despite the distance between them was approx. 7 m.

The clay is covered by fluvioglacial and glacial deposits, also anthropogenic soils of very variable thickness (from several to several dozen meters). This is illustrated by geological cross sections from various regions of the slope (Figure 3). Due to the variability of the geological structure, they can be represented both for the City Centre of Warsaw as well as for the periphery (e.g., the area of Farys Street, according to ref. [17]).

The presented spatial characteristics were later used in the article to determine numerical models of slopes and to analyze the influence of various factors on slope stability.

3 Genetic factors of structural and physical characteristics of tested soils

The physical and mechanical properties of Neogene clays were formed by sedimentation and subsequent

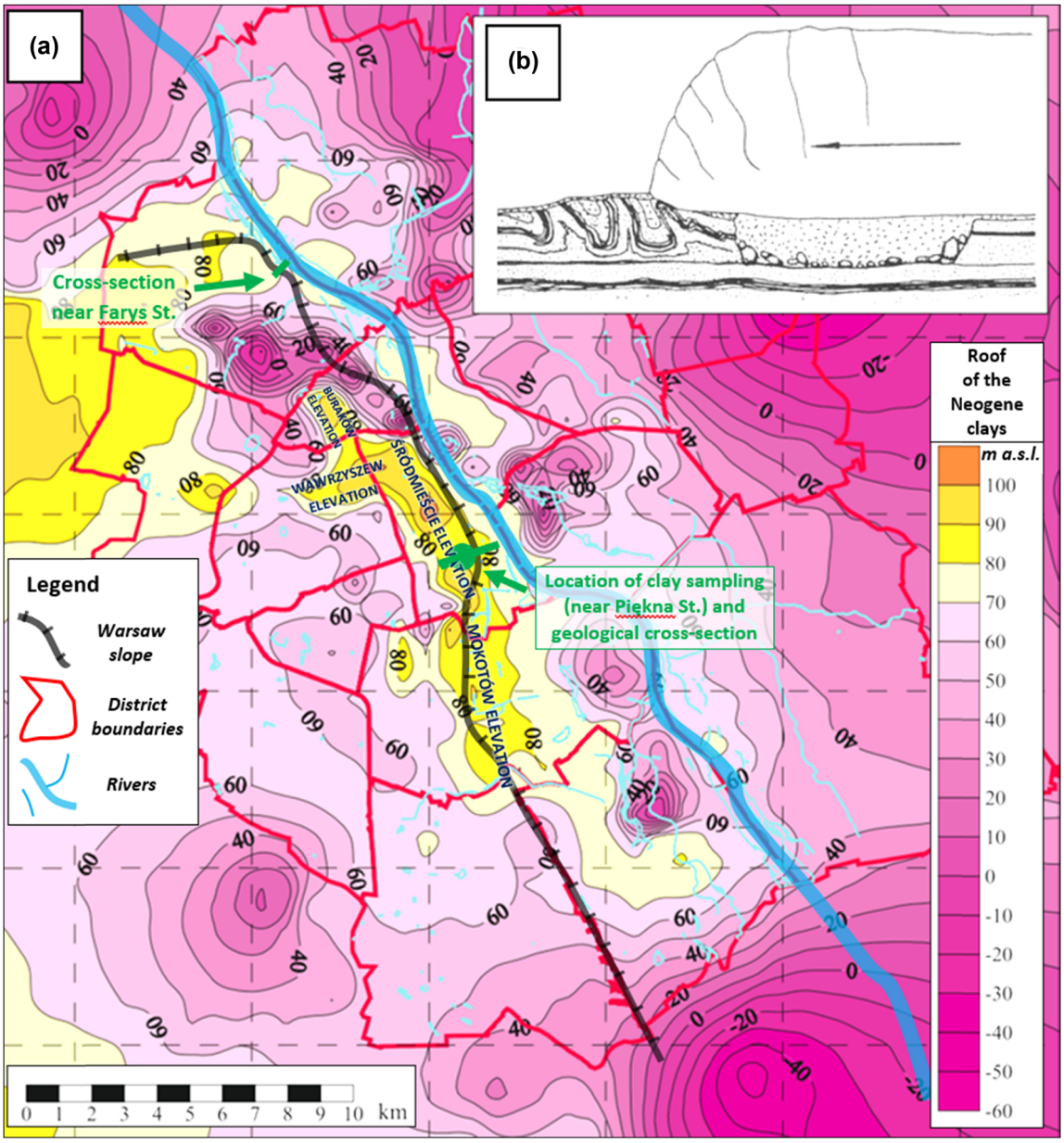

Figure 1: (a) Map of the Neogene clays roof the Warsaw area (modif. after ref. [20]) and (b) Glacitectonic folding mechanism (glacier overthrust front; ref. [48]).

consolidation together with diagenetic processes. In the Quaternary, the glacier that appeared during South Polish, Odra, and Warta glaciation periods covered several times the fine-grained sediments deposited in the Neogene reservoir. The complex history of loads is reflected in the discontinuities and closed cracks observed on a centimeter scale. Several relaxation periods of the subsoil under the glacier were associated with interglacial periods during which both erosion and denudation processes appeared together with alluvial and hollow accumulation. Subsequent loading phases of both Quaternary and Neogene sediments resulted in soil overconsolidation of and quasi-discontinuous deformations. These events resulted in the compaction of the spatial arrangement of the matrix of clay particles and the formation of local microcracks, which were "closed" over time [18]. Microcracks occurring in clay samples create the privileged zones initiating the failure surfaces under deviatoric stress [18]. Such soil structure is more sensitive to changes in moisture [19] due to privileged drainage routes. Structural discontinuities caused by the influence of the glacier may occur down to several dozen meters below the clay roof [2]. The obtained values of the overconsolidation ratio of Neogene clays from Warsaw determined on the basis of the CPT test results were in

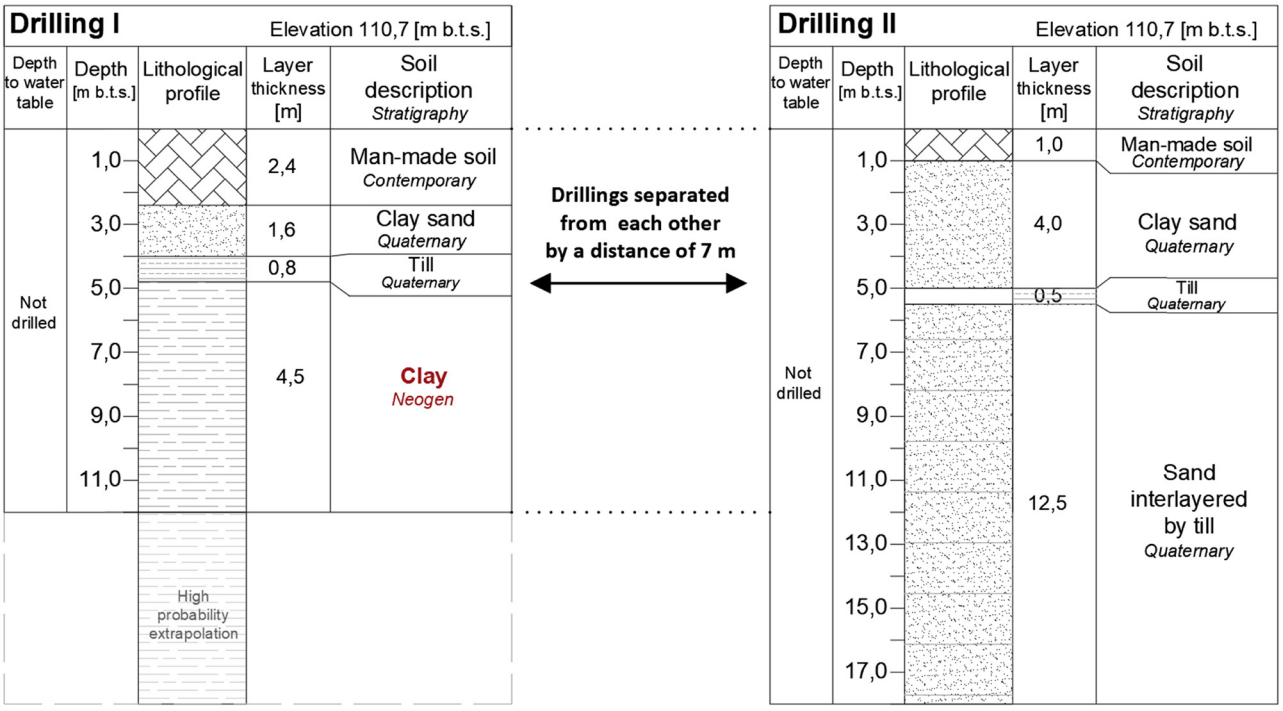

Figure 2: Examples of two lithological profiles drilled near the sampling site.

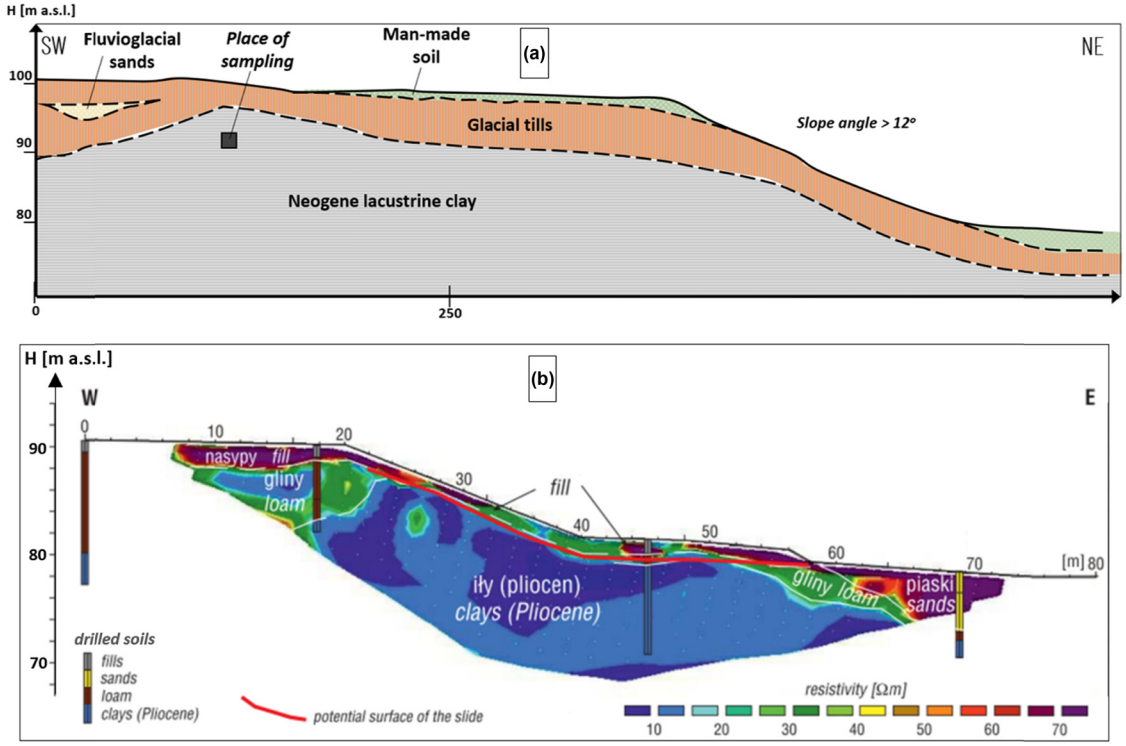

Figure 3: Forms of Neogene clay roof in the Warsaw slope: (a) schematic geological section near the Piękna St. and (b) geophysical cross section at the Farys St.; (modif. after ref. [17]).

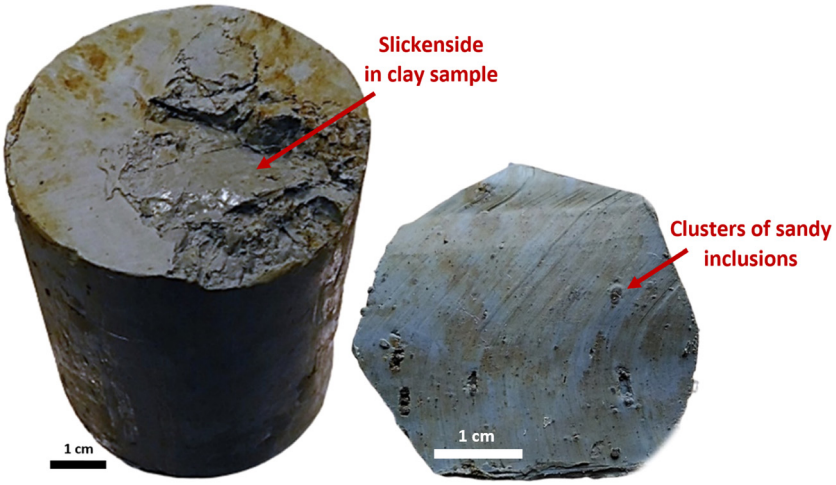

Figure 4: Neogene clay from Warsaw Śródmieście district (near Piękna St.) with macroscopically visible structural elements.

the range of 6.2–12.5, with the mean value of 9 [20], and the earth pressure coefficient at rest K_0 = 1–1.3 [21].

The clays sampled at a depth of 10 m from the area of Piękna Street (City Centre) had a dark gray color, locally black or green, which indicated the diversity of mineral composition of tested soils. Inclusions of the sandy and silty fraction were rich in iron. During cutting cylindrical specimens for the triaxial test, small-scale shears were observed, as well as microfaults (dozen millimeters), becoming visible during the drying of the fresh surface of the specimens (Figure 4).

The values of the physical parameters of tested soils matched the ranges of regional characteristics obtained by other authors [2,20]. The results of the physical properties of the research material versus the synthetic characteristics of the clay formation from the Warsaw region are shown in Figure 5.

According to the ISO 14688-1 standard [22], the investigated soil was classified as clay (Cl). The X-ray structural analysis showed that beidellite was the main component of the clay fraction, as illite and kaolinite were of secondary importance. Similar characteristics were obtained from the study of Neogene clay from Warsaw in refs [11,14]. The natural water content of the collected samples was similar to those fully saturated, which was associated with the presence of soil in the saturation zone – below the Quaternary groundwater table. Due to pre-consolidation, these clays were also stiff.

4 Methodology of laboratory tests

The purpose of the laboratory test program was to assess the creep effect on changes in the shear strength of studied soils. The stepwise procedure for this task is illustrated in Figure 6.

The main aspect of the program was to compare the behavior of soil samples sheared during a continuous increase of deviatoric stress with the results of tests in which shearing was preceded by a creep stage under constant load. Reliable comparison depends on the selection of samples with the most similar structural characteristics. This similarity was determined by means of imaging the internal soil structure by preliminary densitometric evaluation of the cores and then the use of computed tomography on samples prepared for triaxial testing (point I of the procedure).

Samples with similar structural features were divided into two groups intended for the implementation of

Parameters		Tests results compared to archival studies of the Neogene clays formation [2], [20]
Fraction [%]	<2 µm	30 **45** 56
	2-50 µm	37.5 **41** 50
	>50 µm	6.5 **14** 20
Bulk density, ρ [g/cm^3]		1.8 **1.98** 2.23
Porosity index, e [-]		0.28 **0.68** 0,92
Water content, w_n [%]		19.2 **26** 35.6
Liquid limit, w_L [%]		30 **76** 115
Plastic limit, w_P [%]		15 **35** 40
Plasticity index, Ip [%]		15 **41** 75
Skempton's activity, A [-]		0.75 **1.16** 1.5

Figure 5: The physical properties of the Neogene clay against archival results – ranges of regional variability.

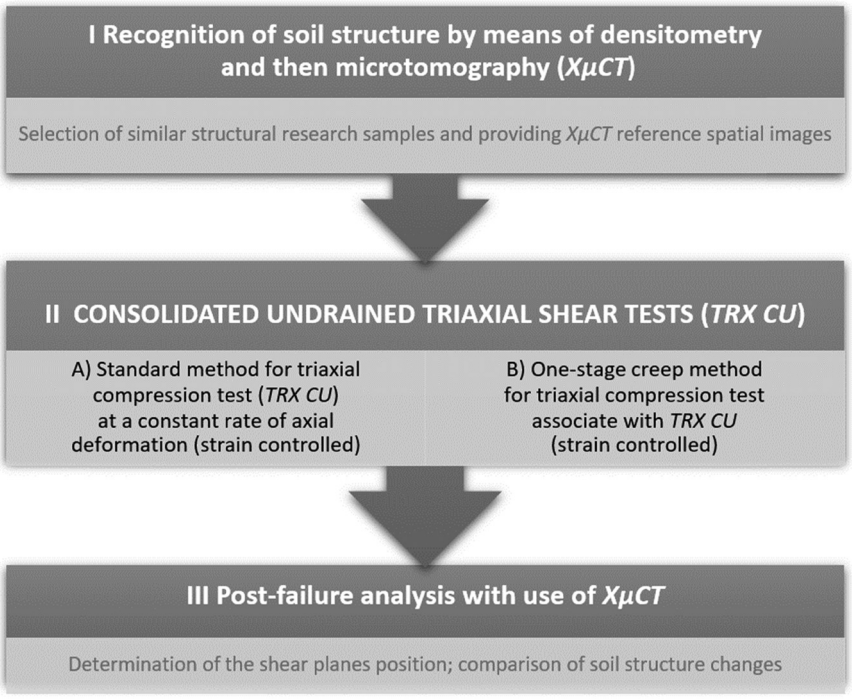

Figure 6: Scheme of laboratory test focus on creep process impact on Neogene clay strength.

separate research scenarios. The samples of the first group were intended to determine the shear strength of soil in the TRX apparatus under continuously increasing load (point IIA of the procedure).

The obtained shear parameters allowed to determine the 60% value of the non-destructive deviatoric stress ($q_f = \sigma_1 - \sigma_3$) at which the creep tests ($q = 0.6q_f$) were supposed to be carried out using the second group of samples with similar structural characteristics. These samples were subjected to triaxial compression tests with a modified loading program (point IIB of the procedure). After the initial continuous increase of deviatoric stress, several days, the constant axial load was applied, to observe the soil creep. Then, the increase of load was resumed, controlled by the condition of constant axial displacement, until the samples lost their shear strength and failure appeared.

After the shear and creep tests, the samples were again subjected to tomographic structural imaging (stage III) to assess the changes resulting from the deformation and shearing of soils.

4.1 Soil structure recognition

The preliminary assessment of the soil structure before its removal from Shelby samplers was performed using X-ray densitometry. Using this method, the soil inside two metal samplers was tested. The passage of X-rays through the thin metal walls of the sampler caused a constant error in registering the soil material density value; however, a qualitative characteristic of soil density variation was obtained without the risk of structural changes during the extrusion of the soil material from the sampler. This allowed indicating the zones of structure disturbance along the core. The obtained densitometric images had low resolution (pixel size ~1 mm), so the boundaries of zones with various densities were blurred. On the other hand, in a short time of exposure (~30 min), it was possible to identify hidden zones of the loosened material and select the appropriate parts of the core for cutting cylindrical samples (h = 72 mm in height and d = 36 mm in diameter) oriented with a vertical axis in accordance with the natural orientation of the soil substrate.

Then, the samples for strain and strength tests in the TRX apparatus were subjected to microtomographic imaging according to the methodology in refs [23–25]. A MicroXCT-400 model, produced by the American company Xradia, was used. X-ray high-resolution computed microtomography tests (XμCT) included the following: data recording at different directions of exposure, their assembly as several series of projections, image processing, and final three-dimensional visualization. The exposure time of a

single image was 6 s. A series of 1,024 X-ray images of each sample (in the format of 8-bit BMP images with a resolution of 1,024 × 1,024) was obtained.

The obtained images showed the variability of the coefficient of X-ray absorption, influenced mainly by the density variation of the solid phase of the clay material. The most compacted areas were characterized by lighter shades, while the darkest areas were recognized as gaps, often filled with loose materials.

During the exposure, the soil samples were protected with a rubber membrane, which eliminated the possibility of water evaporation. Due to the low density and membrane thickness in comparison to the size of the soil sample, it did not significantly affect the quality of radiographs. With the assumed cylindrical dimensions of the samples, pixels with a side of ~40 μm were obtained. To assess the possibility of imaging quality improvement, several additional exposures of smaller, centimeter fragments of clay samples were carried out. The imaging of structural discontinuities affecting the deformation of the soil was therefore fully sufficient when using the above-mentioned exposure parameters. On the other hand, the ranges of pore size of the analyzed clays, determined by SEM, often presented in the literature, were several dozen times lower (0.75–1.90 μm; ref. [2]). The SEM method, due to the small size of the scanned surfaces and obtaining 2D images, is not as comprehensive in the assessment of structural discontinuities as the presented microtomographic imaging.

4.2 Shear strength tests

Shear tests have been performed with the use of triaxial systems, based on computer control and data acquisition by GDS Instruments equipment and software solutions. A general methodology of triaxial tests was consistent with current standards [26], and state-of-the-art practices were described in refs [27,28], with some unique addition.

Preparation of test samples for both standard shear strength determination (the names of the samples S_1, S_2, S_3 referred to the first letter of "shearing") and tests with additional consideration of the creep stage was preceded by uniformly adopted saturation conditions.

According to the commonly known and established practice, preparation of the samples included saturation by backpressure technique [29] and isotropic consolidation. Backpressure value used to achieve demanded saturation level (the end saturation criteria were B values, which were ~0.84, which refers to the research of ref. [30] was up to 800 kPa. Effective consolidation stresses applied to the samples in one series were σ'_3 = 100, 200, and 300 kPa (the consolidation took up to 3 days). These values represent the general stress state, water level depth, and depth of sampling.

The samples were subjected to appropriate strength tests at increasing stress σ_1 automatically adjusted to the assumed, previously calculated as appropriate, constant displacement rate vs = 0.01 mm/min.

These studies were conducted under undrained conditions (CU). This test type has been chosen, as representing a more critical scenario of subsoil conditions, giving insight into pore pressure behavior, resulting in effective strength parameters, and also being more time efficient in comparison to the CD test. The deformation increase observed in the CU tests depends on the load as well as on soil reaction by changes in soil porosity, without the parallel participation of filtration and consolidation processes. On the other hand, in the case of CD tests (drained), these processes cooperate, causing changes in the character of deformability and strength. The significance of these factors has been repeatedly assessed by analyzing various results of drained and undrained triaxial tests. For example, in normally consolidated clays from the Macao region of China, ref. [31] obtained higher deformation values and higher soil strengths from drained tests than in undrained ones. These effects were associated with the influence of filtration and consolidation processes. Therefore, the analysis confirmed that the CU were more unfavorable and, therefore, much more safe in engineering predictions.

The effective values of internal friction angle and cohesion were determined according to classical methodology resulting from the Coulomb–Mohr theory [32]. For the representation and analysis of the results, standard MIT stress path parameters [33] have been used, i.e., mean effective stress $s' = (\sigma'_1 + \sigma'_3)/2$ and shear stress $t' = t = (\sigma'_1 - \sigma'_3)/2$, which is half of the deviatoric stress q. The maximum value of the deviatoric stress was considered as shear stress criterion.

The obtained values of the internal friction angle were also compared with the shear angles (θ) of the samples determined after the shear tests completion based on the analysis of the directions of the shear surfaces in the microtomographic images. The theoretically specified shear angle in a homogeneous material should be $\theta = 45° + (\phi'/2)$. Deviations from this principle may indicate the heterogeneity of the soil material, as well as structural features as microcracks and sedimentation lamination [34,35].

Other results of the study of overconsolidated clays from the Lower Silesia region [35] also showed lower than

theoretically expected values of θ. These effects were explained by reactivating discontinuities or weak zones in the soil structure. Their presence in some samples resulted in decreasing the shear angles in comparison to the theoretical ones. This comparative approach has also been used in interpreting the research presented in this article.

4.3 Triaxial creep tests

The creep tests conducted on the second group of samples (the names of the samples C_1, C_2, C_3 referred to the first letter of "creep") were planned with the stress level (SL) = q/q_f = 0.60, i.e., 60% of the expected maximum deviatoric stress (q_f). Then, changes in the axial deformation (ε_1) were observed for 14 days as a function of time, and then, the load was continuously increased until the failure was achieved. The choice of the vertical stress value at which creep observations were made may be optional, but usually with the recommendation that creep should be declining, i.e., it does not lead directly to loss of soil strength. The value of SL = 0.6 adopted in this study was determined on the basis of the results of authors' experiments [23] and the works of ref. [36], where decelerating creep was observed at stresses 30 to 70% of the maximum deviatoric stress ($\sigma'_1 - \sigma'_3$). Triaxial stress is an important aspect of creep studies [37]. In the following research, the expected values of the maximum deviatoric stress at failure were determined based on the results of standard triaxial CU tests of the first group soils that had the same lithogenetic type and structure. The maximum deviatoric stress in the tests of the second group soils (q_{max}) obtained after the completion of the creep stage and re-application of the constant load increase may differ from the reference results from the soils of the first group (q_f). It was conditioned by the natural structural differentiation of the studied soils as well as by the influence of the previous creeping. The analysis of these differences is one of the goals of research and analysis.

The creep of the investigated soils was characterized based on changes in the increment of axial deformations ε_1 as a function of time t. Resulting from the analysis of the equation (ε_1) – log t, three qualitative types of deformation changes might be distinguished: decelerating, quasi-steady state, and accelerating. Hence, for the quantitative characterization of the creep behavior in any time interval, a dimensionless parameter m was adopted [38].

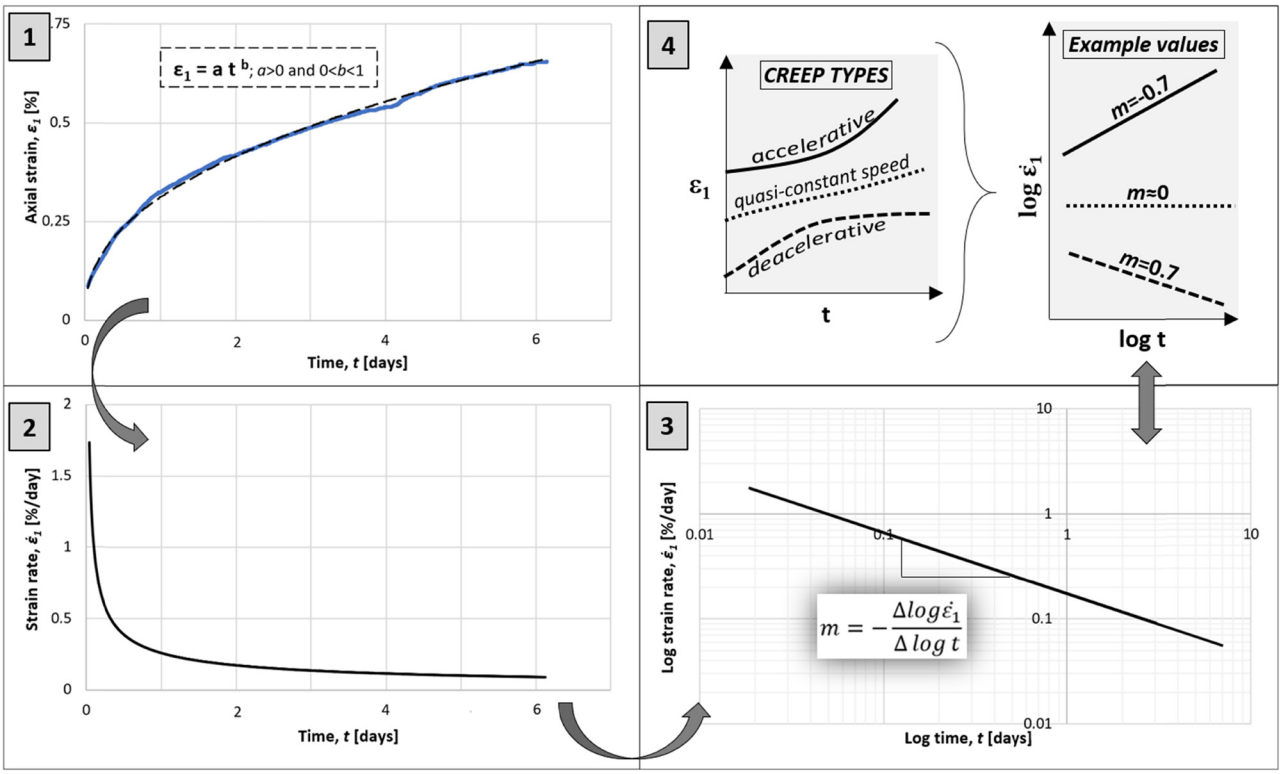

Figure 7: Calculation scheme of parameter m and its various values in relation to the character of the strain rate increase.

$$m = -\frac{\Delta \log \varepsilon_1}{\Delta \log t}[-]. \quad (1)$$

The parameter m is based on the model assumption of logarithmic linearization of the increment in axial deformation as a function of time. The decreasing velocity of deformation corresponds to the value of $m > 0$ (decelerating creep). As the load increases, the soil shows a constant rate of deformation, which corresponds to the value of $m = 0$. The value of $m < 0$ corresponds to the increase in the rate of deformation that occurs directly before shearing.

Figure 7 shows a scheme for determining m value, comprising, in turn:

1) Registration of vertical deformations as a power function of time $e = at^b$, if $a > 0$ and $0 < b < 1$, the deformation has a decelerating character (Figure 7.1).
2) A power approximation of the deformation velocity versus time, at a decelerating creep $a > 0$ and $b < 0$ (Figure 7.2).
3) Logarithmic linearization of deformation velocity versus time (Figure 7.3).
4) The relationship between the types of deformation changes: decelerating, quasi-steady state, and accelerating, and the m values: positive, zero, and negative (Figure 7.4).

When discussing the determining m parameter, it is necessary to explain the assumption of the axial strain rate ε_1 as the creep indicator, despite the triaxial conditions of changes in stress and strain. Ref. [39] showed that the m parameter values calculated on the basis of ε_1 were close to those determined based on the volumetric deformations ($\varepsilon_V = \varepsilon_1 + 2\varepsilon_3$). At the same time, ref. [40] noted greater uncertainty related to the possible use of ε_V than ε_1.

5 Results and discussion

5.1 Structural evaluation of tested samples

The purposes of densitometry and computed microtomography research were as follows:

- The assessment of the character and the origin of structural discontinuities of tested soil;
- The selection of samples with similar structural characteristics for comparative rheological and strength tests;
- The assessment of the impact of loads applied in triaxial tests on forming the new structural effects.

The results of low-resolution exposures performed in the densitometer allowed to obtain the preliminary assessment of the structural condition of the cores inside Shelby samplers. The observed disturbances may result from both the drilling and sampling techniques and the natural genetic features of the soil. The dark zones visible in the density images indicated a significant relaxation and even voids (Figure 8). These parts of the core (intervals: 9.12–9.20 m and 10.65–10.95 m below the ground level) were eliminated from further research. Taking the remaining material into consideration, cylindrical soil samples with standardized dimensions (36 mm × 72 mm) were prepared. Before placing them in the triaxial apparatus, microtomographic exposures were performed. This way, spatial data with ~25 times (and in single XμCT scans even ~60 times) better resolution were obtained. The possibility of creating any digital cross sections on their basis enabled a multi-directional analysis of the structural variability of the material selected for further research.

Structural images of soil samples for TRX tests indicated the diverse nature of the recorded heterogeneities.

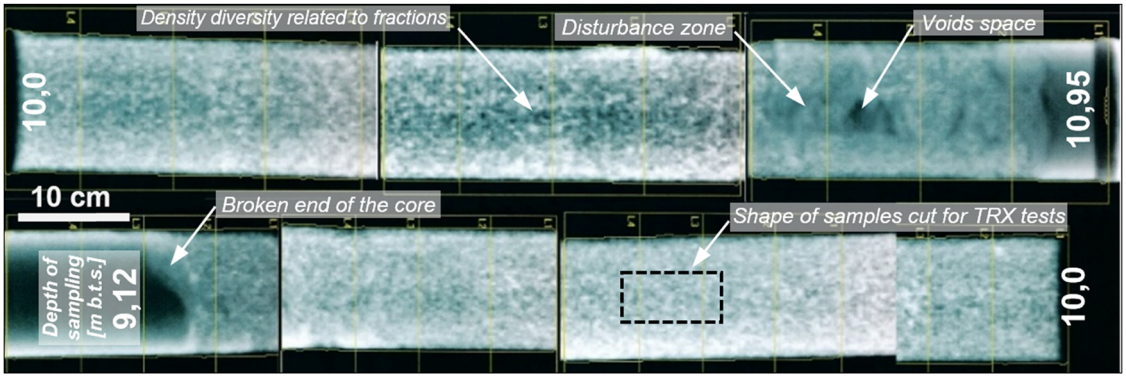

Figure 8: Interpretation of the densitometer imaging results of the analyzed clay in Shelby probes.

For example, the image of the U_1 sample (the name refers to the sampling sites, i.e. U as upland) showed extensive, darker fragments of lower density, corresponding probably to sandy inclusions (Figure 9). This indicated the variability of the genesis and transfer of the material even at a small scale. On the other hand, microcracks and

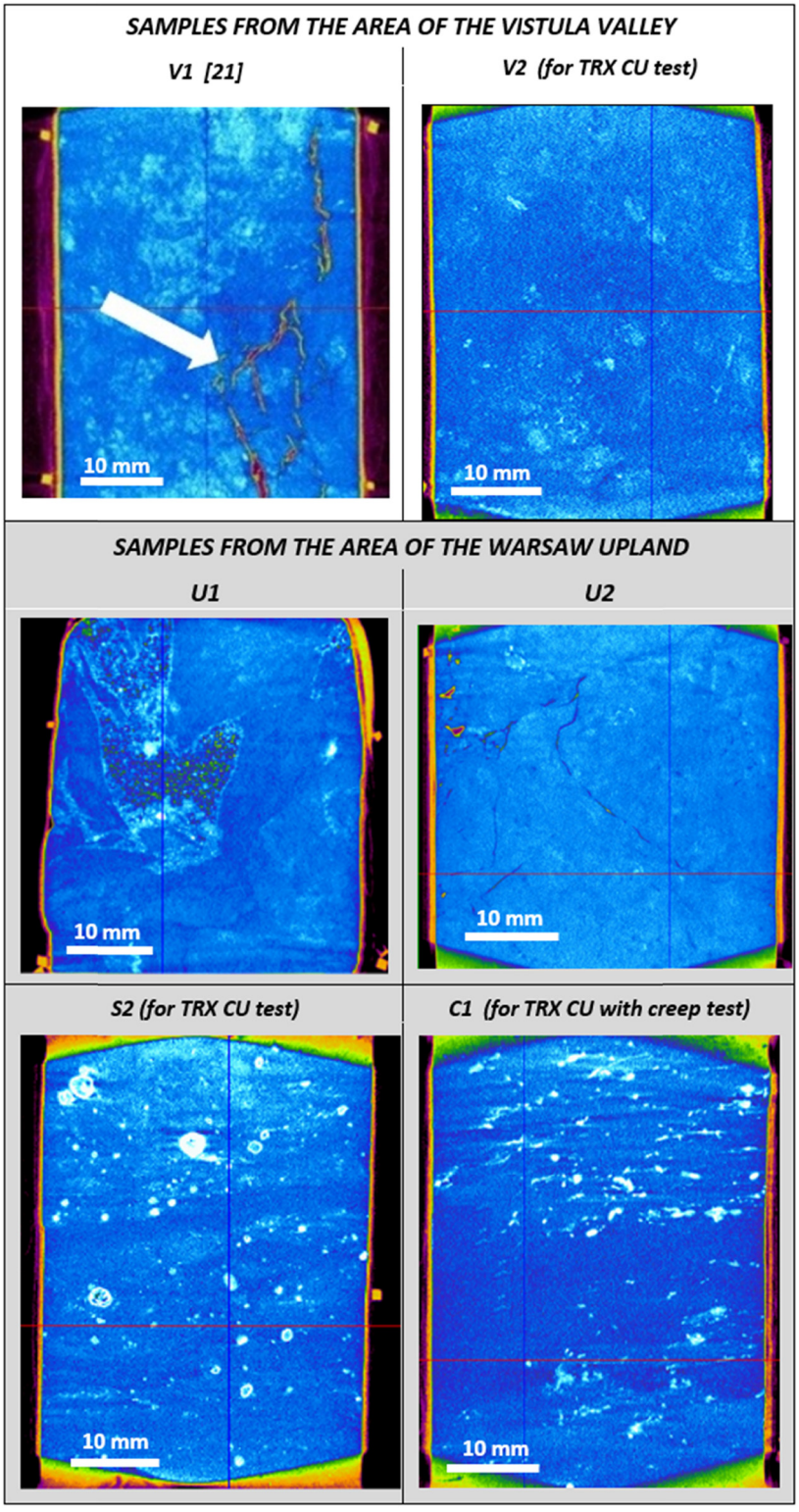

Figure 9: The compilation of various images of the Neogene clay from the area of Warsaw slope.

voids found in the sample U_2 (Figure 9) were considered to be related to the complex stress state due to glacitectonic strains. Some cracks may show up and develop additionally during soil sampling and/or during extruding it from the sampler and preparing cylindrical samples. A similar genesis of discontinuities was observed in sample V_1 (the name refers to the sampling sites, i.e. V as valley; Figure 9), collected from Powiśle [23], where in V_1 sample, the cracks with an opening of up to several millimeters and a few centimeters long were observed. These examples showed that structural disturbances may appear at various stages of sediment formation and transformation as well as during the collection and preparation of samples for testing. The character and conditions of structural variability may significantly affect the separate, individualized deformation and strength behavior of samples. Hence, the presented samples U_1, U_2 were not qualified for further triaxial tests, as they did not meet the condition of structural similarity to other samples designated to shearing tests series (S_1, S_2, S_3) and creep test series (C_1, C_2, C_3).

Exemplary microtomographic sections of the chosen for further triaxial tests samples (V_2, S_2, and C_1) are shown in Figure 9. They illustrate typical images of the internal structure, i.e., a relatively homogeneous clay material with a dispersed content of silty fraction, without microcracks visible at the resolution used. Among other

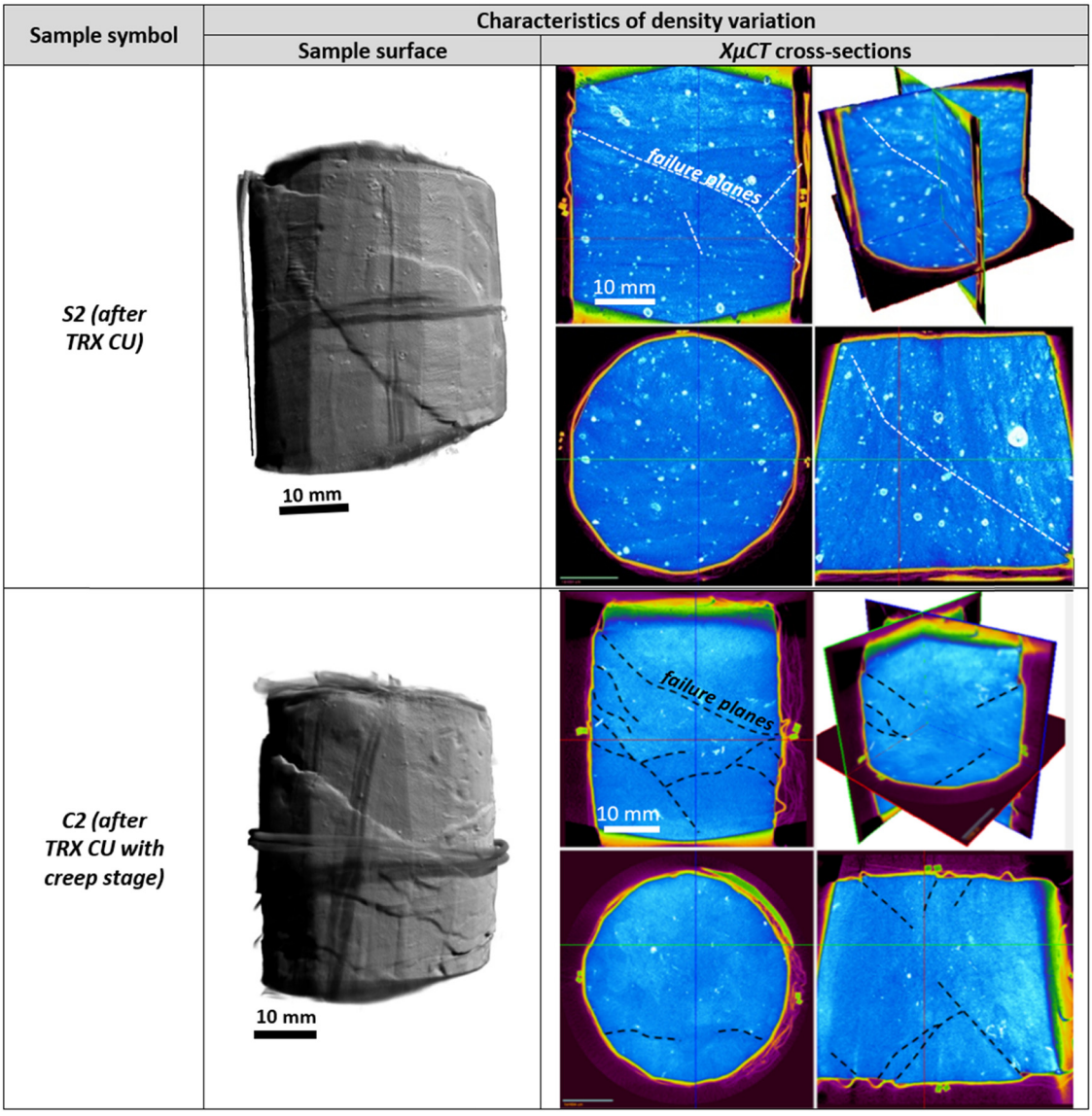

Figure 10: Exemplary images of the post-failure structure of Neogene clay samples (after triaxial tests).

structural features, it is worth mentioning that the "nest" clusters with lighter shades indicate a higher density of the soil material. They may indicate the presence of iron compounds (with higher density in relation to the clay matrix). Such effects were found in small sandy enclaves accumulating the mineralized liquid phase in the pore space. The presented interpretations were verified and confirmed directly by cutting the samples after performing triaxial tests and repeated microtomographic images. Characteristic aggregates of sand grains with a rusty color suggesting the presence of iron ions in the third oxidation state were identified.

The examples of the images of the microstructures of Neogene clays after the TRX CU tests (Figure 10) clearly reveal both the shear surfaces and the zones of plastic displacement inside the samples. This indicates a mixed, brittle-plastic mechanism of deformations.

A similar character as well as lithological and structural changes was noted in microtomographic images of samples subjected to the creep stage and then shear (C_2 – Figure 10).

The complementary use of densitometry and microtomography indicates their universal, innovative application in initial quality recognition of full-size soil core and subsequent, detailed structural analysis.

5.2 Shear strength

The shear strength (Table 1) shows some differences when comparing the two groups of test samples with the standard continuous load increase (samples S_1, S_2, S_3) and with a gap during continuous loading, at which long-term creep at constant stress was monitored (samples C_1, C_2, C_3).

The summarizing data and the obtained results are presented in Table 1 characterizing:

- Conditions of initial consolidation;
- Axial deformations and stresses s' and t (deviatoric) at failure;
- Cohesion and internal friction angle;
- Shear angles determined on the basis of the tomographic images.

In general, despite careful selection of structural similarity, the tested samples showed some differentiation in behavior. It was confirmed by the random variability of the consolidation coefficient in the range $(0.6–5)\,10^{-9}$ m^2/s. It was probably conditioned by local changes in water content and pore pressure distribution.

Figure 11 shows the results of all shear stages of the tested samples using graphs of principal effective stress ratio (σ'_1/σ'_3) against the axial strain and pore pressure changes. After the 14-day creep stage, the maximum deviator was most often achieved faster than in the standard triaxial tests. In comparison to the standard tests, the samples of the "C" series show an increase of s' and t values at failure. For the sample consolidated at σ'_3 = 100 kPa, the increase of s' was 32% and the deviatoric stress t was 72%. For σ'_3 = 200 kPa, an increase was as follows: s' = 23% and t = 36%, while at σ'_3 = 300 kPa, 24 and 20%, respectively. Linear strength envelope interpretation of "C" test gives as a result higher angle of internal

Table 1: Characteristics of the course and results of shear strength tests of Neogene clay samples

Sample symbol	Selected parameters of *TRX* tests						Interpretation of the *TRX tests* results		
	Consolidation stage		*Shear stage*				*Strength parameters*		
	Final eff. consol. stresses σ_3' [kPa]	Coefficient of consol. c_v [m^2/s]	Max. deviatoric stress q_f [kPa]	The average effective stress s' [kPa]	Stress levels based on *TRX* with creep tests SL_{cr} [-]	Axial strains at the moment of failure ε_f [%]	Internal friction angle ϕ' [°]	Cohesion c' [kPa]	Inclination angles of the failure planes determined from the *XμCT* analyzes θ_{cr} [°]
S1	100	*5.0·10^{-9}*	*94.2*	*98.7*	0.45	*0.9*			*~45*
C1^		1.1·10^{-9}	124.2	169.5		2.3			9.5-<u>48.6</u>
S2	200	*6.0·10^{-10}*	*161.2*	*216.8*	0.49	*4.0*	*17.5*	*17.8*	*~51*
C2		3.2·10^{-9}	198.0	294.1		1.7	21	0	15.3-<u>47.8</u>
S3	300	*1.6·10^{-9}*	*210.1*	*291.0*	0.48	*5.0*			*39-54*
C3		1.8·10^{-9}	260.0	350.4		1.8			16.7-<u>47.0</u>

The values in grey refer to the results of standard TRX CU tests preceded with analogous consolidation conditions.
<u>The underlined angle values</u> indicate the dominant failure plane.
^The use of weights.

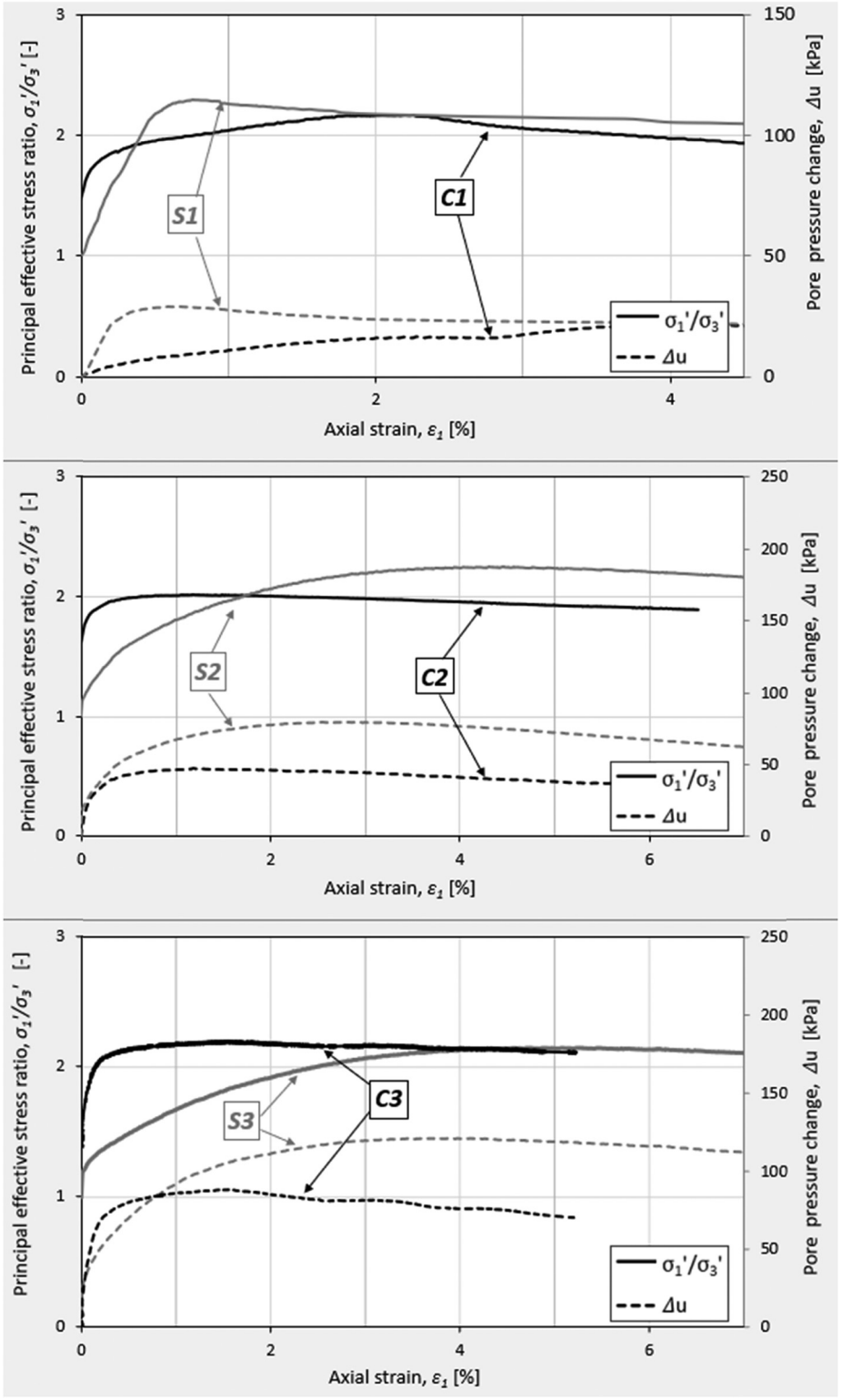

Figure 11: Comparison of the shear stage of two exemplary triaxial tests: standard shearing (S1–S3) and taking into account earlier creep (C1–C3).

friction (20% increase comparing to "S" test) and cohesion reduced to zero (Table 1). A possible explanation of the reduction of cohesion is creep-reactivated microdiscontinuities related to the glacitectonic history of the sediment. Due to a limited number of samples available, authors cannot draw firm conclusions, although a very thorough examination

of the tested material prior to the test gives confidence toward strength parameters obtained.

The variability of the cohesion and the internal friction angle of Neogene clays from Warsaw maybe quite significant [2] – Figure 12, which results from the structural conditions related to the specific sedimentation and glaciotectonic history. This is typical for Polish Neogene clay sedimented in various places like the Bydgoszcz region where its variability is even higher [41]. The soil structure with fissures determining soil strength can be observed also in similar London clay [19,34]. The samples analyzed in this article were characterized by high values of internal friction angle, similar to the upper estimates for the Neogene clays from Warsaw and relatively low values of cohesion, even reduced to zero in the soil weakened by the creep stage.

Comparison of the character of deformations and the failure conditions of tested soils with data from other regions allowed to assess the determinants of deformations. As a reference, it can be assumed from ref. [27] that for plastic clays, strain at failure is from 15 to 30%. Hence, in the pre-consolidated formations, these values maybe even five times lower. For example, for the Neogene clays located to the south of Wrocław, a range of strains 3–6% have been reported [42]. From the analysis of glacitectonically disturbed Neogene clays from Warsaw, comparable 1–5% strains at failure were observed. Similar results can be found in other publications [43]. Low values of axial strains at failure were associated with their stiff, pre-consolidated structure, and the probable initiation of shearing along glacitectonically disturbed weak zones and microdiscontinuities.

An important piece of evidence indicating the role of weak surfaces connected with the history of loads on the strength characteristics was the comparisons of shear

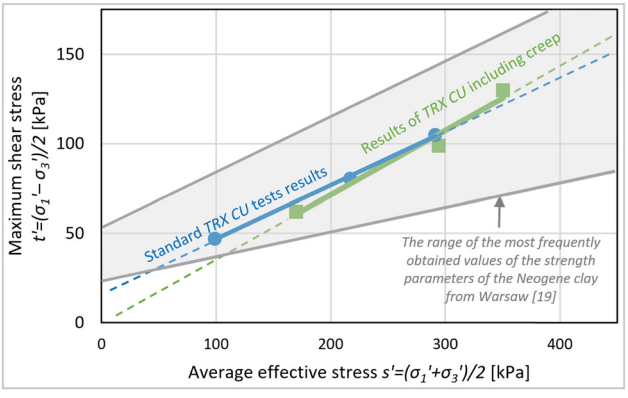

Figure 12: Failure envelopes for two series of triaxial compression tests (standard and including creep stage) against the range of archival test results.

angles in the samples θ_{cr} (after tests with creep stage) and θ_{sh} (after standard TRX CU) with the expected values according to the theoretical Coulomb–Mohr model. The most common values obtained during the research were $\theta_{cr} < \theta_{sh}$ (with the lowest angles from 35 to 9.5°). It proves the structural heterogeneity of the tested material and the role of local microshears in shaping the steady-state states and the conditions for achieving the maximum shear resistance. This explanation corresponds to the abovementioned relations between the microstructural features and the mechanical properties of the soil.

Complementary strength tests extended for creep stage with documentation of microstructural changes is a novel and comprehensive approach. Creep impact on mechanical properties of soil is constantly an explicated issue, where latest studies of stiff clay concern time and stress dependents, e.g., ref. [44].

5.3 The course of clay creep

The evaluation of the creep influence on the strength properties of soils requires a comparison of the course of tests under continuous load increase ("S" tests – shearing on group I samples) with tests where a 14-day creep stage under a constant load was carried out ("C" tests – creep on samples group II). The SL was supposed to correspond to 60% of the maximum (at failure) stress deviator q_f. The values of q_f were assumed on the basis of the shear strength obtained from the "S" tests on the group I samples. The assumed loads were equal only in the range from 45 to 49% of the real value of the load at failure which was achieved later (for group II samples). Thus, the values of q_f obtained from the "C" tests on group II samples turned out to be about 20–30% higher than the results obtained in the "S" tests carried out on group I samples. It was difficult to decide whether the increase in the value of the stress at failure was caused by the structural reconstruction during the decelerating creep. It should be noted that such relations occurred consistently in tests of samples carried out at stresses σ_3 equal to 100, 200, and 300 kPa carried out on the samples of overconsolidated soils.

Characteristics of the creep course and the rate of deceleration depend on the stress which the soil is subjected to and on the individual structure of the samples. The graphs presented in Figure 13a show that the values of the vertical strains were inversely proportional to the horizontal stresses σ_3. These effects are connected with the well-known soil mechanics relations between the compressibility in the triaxial and uniaxial deformation

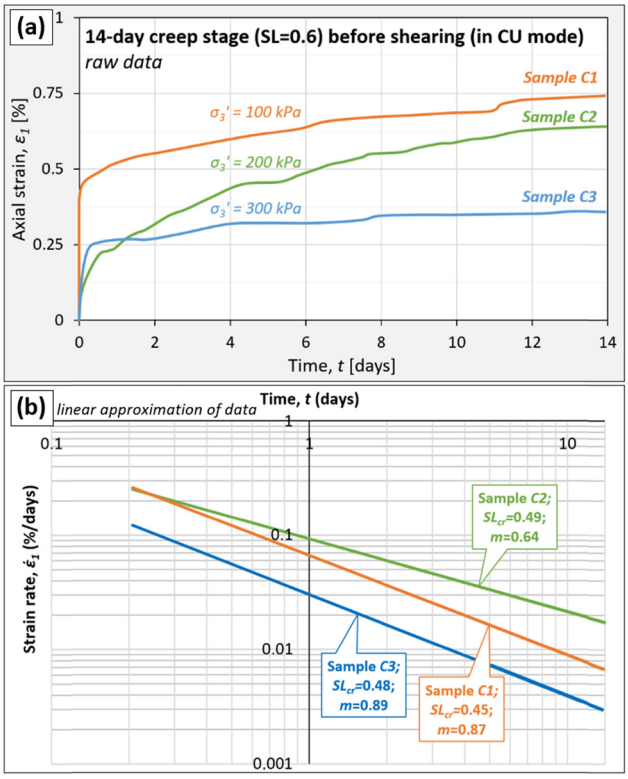

Figure 13: Results of single-stage creep presented as (a) increment of axial strain as a function of time and (b) strain rate as a function of time in logarithmic scales.

state. The decrease in the vertical displacements values was directly related to the limitation of deformations in the horizontal direction caused by the magnitude of horizontal stress applied. This dependence indicates that together with depth, the creep tendency as well as the range of creep deformations preceding soil shearing will be smaller and this refers also to the slopes. This was confirmed by a number of field observations and inclinometric measurements. The one exception may be the presence of visible or hidden structural discontinuities constituting privileged zones of increased deformation of a separate nature.

The course of the creep expressed by the graph shape can also be associated with the structural variability. In comparison to other tests, the C_2 sample tested at σ_3 = 200 kPa showed the highest rate of deformation, which was maintained over several days (Figure 13b). The initial slight deformations did not show a quasi-stabilization, but they systematically developed (up to the highest value observed in the studies considering creep – Table 1), which may result from the natural structural variability, including local changes of state or particle size distribution.

The differences in the creep behavior were reflected in the values of m parameter (Figure 13b). The lowest value of m = 0.64 corresponded to the creep of the above-mentioned C_2 sample. Potentially, in a soil characterized by decreasing values of m parameter, slow but constant displacements on slopes might be expected (i.e., the lowest rate of loss of displacement velocity of the soil of C_2 character among all other samples). If the soil material has no weakening zones, and the load values are about 40–60% of the shearing stress, after the initial significant deformation, the reduction is observed. The characteristics of the creep velocity changes of tested clays confirmed and extended the results of the analyzes provided in ref. [40], where the values of the parameter m < 1 had been obtained for the overconsolidated soils. Nevertheless, the authors [40] underlay the necessity of creep studies on stiff, overconsolidated soils, because of a small number of tests.

6 Modeling of the stability conditions

The results of the TRX tests were used in numerical modeling of the influence of c' and ϕ' on the slope stability. The determination of the stability conditions was carried out using the $c - \phi$ reduction method presented in ref. [45]. This approach has been implemented in the calculation procedures of the Z_Soil 16.08 software. Iterative search for solutions to equilibrium equations was carried out by means of finite element model (FEM) method. An important reason for the selection of FEM was to determine the slip surface position conditioned by the stress state in the slope and the variability of the strength characteristics of soil layers.

Therefore, this method provides a more adequate assessment of the impact of local geological and engineering conditions on stability than classical solutions with a priori assumed shape of the slip surface (usually circular and cylindrical).

The creation of a calculation model appropriate for the given conditions requires geometric optimization of the shape of finite elements and the position of mesh nodes for which iterative calculations of the equilibrium state were carried out. The created numerical models consisted of 36,475 calculation nodes and 33,000 three-dimensional cuboid elements. The dimensional recurrence of the model allowed to compare the results minimizing the influence of the mathematical variability of their construction. No displacement possibilities along the bottom and vertical borders of the model were assumed as border conditions. The size of the entire model was determined so that the boundary conditions did not affect the internal

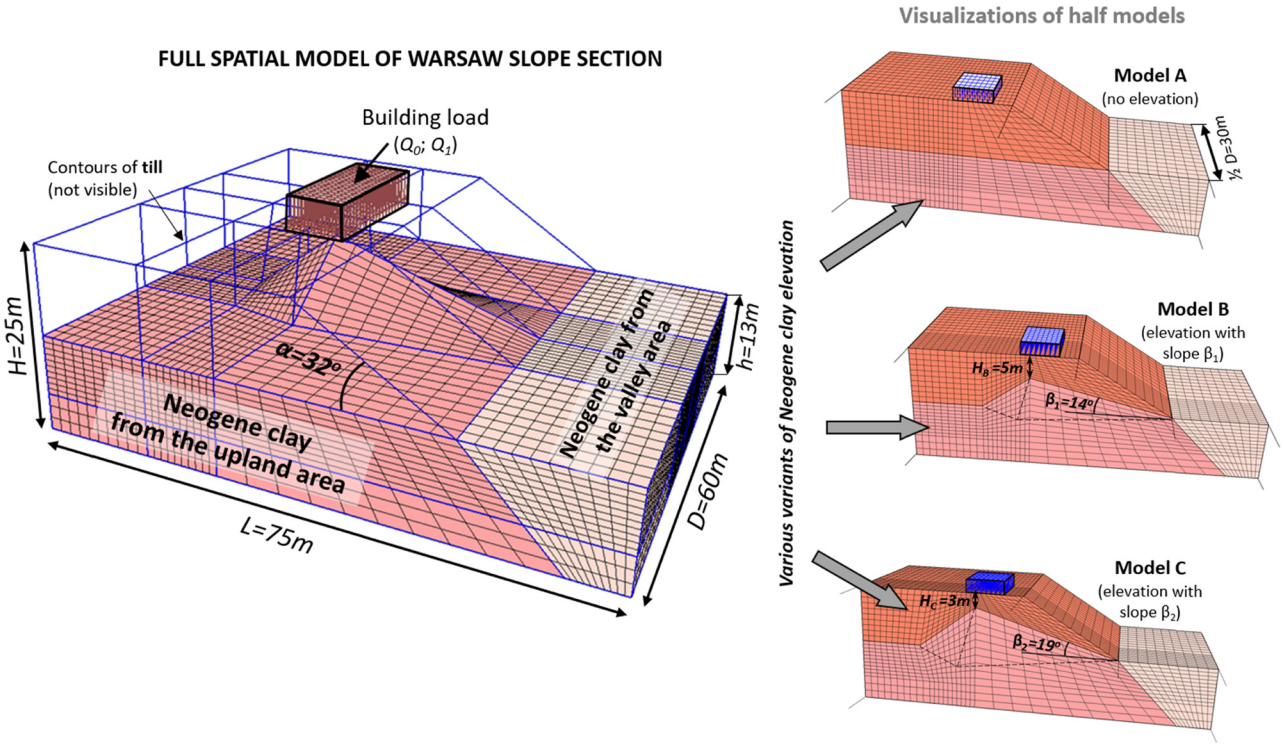

Figure 14: The analyzed models of the Warsaw slope structure.

space of the model, where the zone of slopes and their surroundings was located.

The defined numerical models referred to the nature of the variability of the geological structure in the areas of Piękna Street (Central Warsaw) and Farys Street (Bielany district), adopted on the basis of the works of refs [10,17]. Geological conditions in river valleys are often an inherent feature of slopes determining their geodynamic activity [46].

In the multivariate numerical modeling, the following important factors influencing the stability were considered:

- Position and shape of the boundary surface between Neogene clays (N) and Quaternary glacial tills (Q);
- Optional strength characteristics together with the results of standard tests and tests interrupted by creep;
- Possible load of the slope crown with building objects.

The following models of the position and shape of the boundary surface between the Neogene clays and Quaternary glacial tills were adopted. The (A) model was related to the horizontal course of the N/Q boundary at the base of the model slope. In the (B) and (C) models, the N/Q boundary was formed as a local culmination of clays in the upland base with optional values of slope inclinations along the axis perpendicular to the slope as $\beta_1 = 14°$ and $\beta_2 = 19°$, respectively. The clays within the upland and the slope were covered with a dozen or so meters of stiff, sandy till. To compare the impact of the analyzed options for the slope inclinations on slope stability, the same inclination ($\alpha = 32°$) and the same height ($H = 15$ m) were assumed in all models. The schemes of geological models are illustrated in Figure 14.

Another variable factor affecting the calculations was the influence of the modification of the strength parameters on the slope stability. The sets of values of physical and mechanical parameters of Neogene clays determined on samples from the Warsaw Upland and Powiśle district were used in calculations as well as literature characteristics of stiff, sandy till overlaying Neogene clays (Table 2). The complex and multi-stage formation of the upland (glacitectonics, alternating erosion, and accumulation during successive glacial periods) explains adopting a separate characteristic of the mechanical properties of clays from the upland area, taking the current load of Quaternary glacial tills into account. On the other hand, in the area of the river terraces of Powiśle, the current cover of alluvial and anthropogenic soils was considered as of little importance for loading history of underlying Neogene clays. This was why those sediments were removed from the model.

To assess the impact of buildings in the area of the slopes, possible loads from the construction object on the slope crown were taken into consideration, assuming that:

Table 2: The soil parameters values applied to the numerical models of the analyzed Warsaw slope

Geological formation	Symbol of formation	Physical parameters		Strength parameters		Sources of parameter values
		Water content w [%]	Bulk weight [kN/m^3]	Internal friction angle ϕ' [°]	Cohesion c' [kPa]	
Glacial sandy till from the upland	I	12.0	22.0	22.4	41.7	[2]
Neogene clay from the upland	**IIa**	**27.0**	**19.9**	**17.5**	**17.8**	**Standard TRX CU tests**
	IIb			**21**	**0**	**TRX CU tests including the creep stage**
Neogene clay from the valley	III	26.0	19.8	7.0	25.1	Standard TRX CU tests

Note: The row in bold indicates a formation that is an elevation of clay within the slope.

- The dimensions of the loaded rectangular area were 8 m × 20 m;
- The stress transferred to the substrate was 250 kPa;
- The load was moved 4 m away from the upper edge of the slope.

The model calculations allowed to determine the influence of the assumed boundary conditions on the slope stability. Therefore, according to the diagram presented in Figure 15, the impact of three groups of factors has been taken into account:

– Three models of the geological structure in the slope area (A, B, C);
– Two options for the strength parameters of Neogene clays within the upland (with and without creep influence);
– Two situations: with no load (Q_0) and with load (Q_1) caused by the construction located in the area of the slope crown.

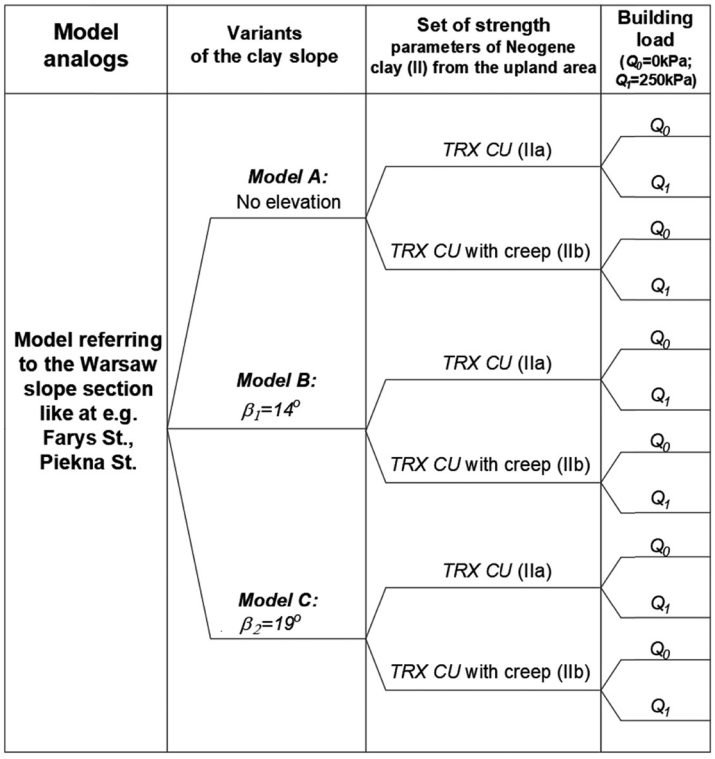

Figure 15: Scheme of multi-variant stability calculations for selected models of the Warsaw slope.

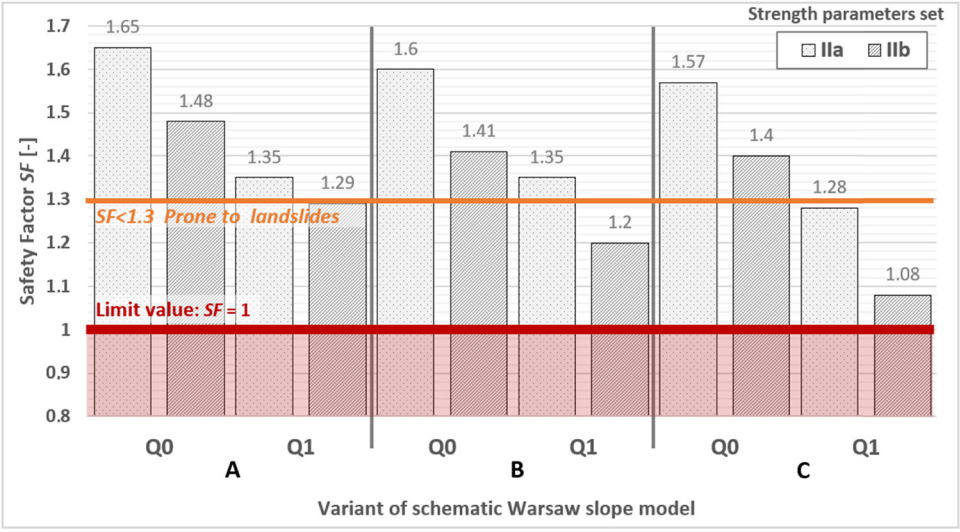

Figure 16: SF results of various variants of the analyzed models.

This gave 12 combinations of boundary conditions. The values of the safety factor (SF) obtained in numerical calculations are shown in Figure 16.

In the analyzed situations, the SF values were in the range of 1.08–1.65. The calculation results taking the acceptable safety margin into account (SF > 1.3) were marked on a colored background. The least favorable combination of boundary conditions can cause as much as 35% reduction of SF value in relation to the most favorable one.

Reference comparisons were made regarding the most favorable conditions: horizontal position of the clay roof, strength parameters determined without the creep stage, and no load on the slope crown.

When analyzing the roles of individual factors, it is worth mentioning that the load caused by the construction gave the most significant reduction in safety. The reductions in SF values in relation to the slope stability without additional load ranged from 13 to 23%. At the same time, the most unfavorable geological situation was the occurrence of the uplift of the Neogene clays roof with a slope of 19° (model C).

Changes in the shear strength of the clay caused by the assumed structural modifications during the soil creep were considered as another factor that reduced the stability index (of about 10–16%). The greatest reduction in SF was recorded in the calculations of the model (C). The characteristic shape of the hypothetical range of geodynamic processes related to the clay uplift is shown in Figure 17.

The assumption of a 14° slope of the clay roof (model B) resulted in decrease only of about a few percent in the SF value in relation to the situation with its horizontal position. These results confirm the observations presented in other articles [19,47] that about 15° slope of the Neogene clays, profoundly affected by fissuring, is long-term stable.

The presented analyses allowed to quantify the impact and significance of individual factors and confirmed the

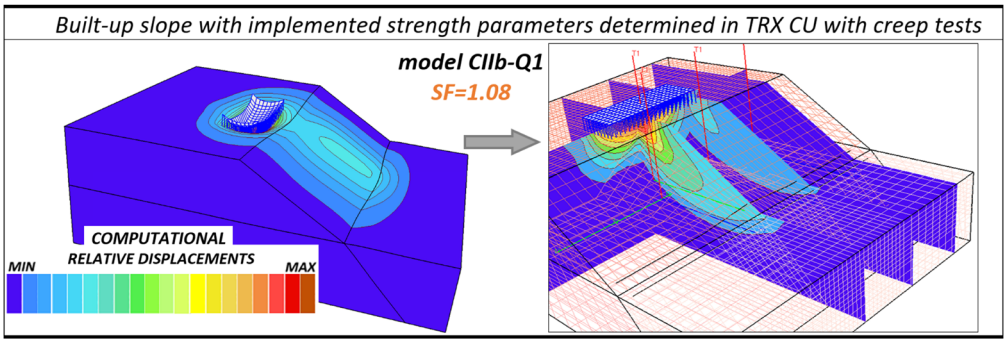

Figure 17: The calculation result of worst-case scenario changes in the stability conditions of the analyzed Warsaw slope models.

validity of optional strength characteristics conditioned by geological history and structural features.

7 Conclusion

Genetically controlled structural features of soils are important factors influencing the reduction of slope stability. Structural heterogeneities, both large-scale and noticeable in several centimeter-long samples, were found in the glacitectonically disturbed Neogene clays from Warsaw. Structural features determined in traditional, macroscopic scale can be spatially and significantly characterized by means of densitometric images and computer microtomography (XμCT). Densitometry with an image accuracy of ~1 mm and a relatively short exposure time (~30 min) provide a non-invasive and non-destructive assessment of the structural condition of the soil cores obtained from boreholes. XμCT technique allowed to observe the more detailed (with accuracy of several dozen micrometers) structural features of tested Neogene clay samples: the compact character of the clay matrix with scattered clusters of silty fraction, as well as closed linear discontinuities recorded as traces of microcracks (fissures) in overconsolidated and glacitectonically disturbed soil. After the triaxial tests (TRX), typically several shear surfaces with the dominant angle of inclination of about $\theta_{sh} \geq 45°$ in relation to the horizontal level were identified, where lower values of the angle θ_{cr} were observed in the tests preceded by the creep stage.

It was investigated that changes in the velocity of soil axial deformation during creep depended not only on the value of the deviatoric stress but also could be caused by even small structural differences of the soil structure. In the studied samples of Neogene clay from Warsaw, the decelerating creep was noted at a constant stress lower than 60% of the shear stress deviator. The observed creep velocity decrease as a function of time is differentiated by the values of the parameter $m > 0$ which on a double logarithmic scale indicates the reduction of the vertical strain velocity as a function of time. The lowest values of m are associated with a smaller reduction of the deformation rate. The creep stage may affect the character of stress and pore pressure changes with a decrease in their values after reaching the limit state (at failure). It was confirmed by a rigid model of strength loss.

Neogene clays from Warsaw are characterized by high variability of strength characteristics. Literature values of ϕ are ranging from 7 to 19° and c ranging from 18 to 55 kPa. Therefore in this study, the obtained values $\phi' = 17.5°$ and $c' = 17.8$ kPa determined from standard tests were located close to the upper values of the internal friction angle and lower values of cohesion. The determination of the shear strength of the samples after former creep stage indicated a further 20% increase in the value of internal friction angle of clay and the loss of cohesion. These results were taken into consideration in the optional selection of parameters for model calculations of slope stability carried out by comparative FEM modeling. The calculated values of the SF were in the range from 1.65 to 1.08, which was dependent on input conditions. The factor that reduced the SF value the most (by about 23%) was the building load where the 19° inclination of the clay roof was assumed. Additionally, changes in the shear strength of clays caused by structural effects of soil creep were considered as the second quantitative factor reducing the stability factor (decrease from 10 to 16%). Referring to the generally large variability of the strength parameters of the overconsolidated Neogene clays, this factor, depending on the location, maybe of much greater importance. Optional modeling of the Neogene clay roof slope indicates on its long-term stable inclination (below ~14°).

Acknowledgments: The authors would like to thank the anonymous reviewers for their valuable comments.

Funding information: This research was funded by the University of Warsaw, grant number DSM 501-D113-86-115600-24-1130300.

Author contributions: Ł.K. is the corresponding author and the lead author of this article. P.D., as interpreter co-author, wrote part of the article and edited it a number of times. T.S. and K.K. as co-authors of this article have reviewed its scientific content and linguistic presentation. All authors have read and agreed to the published version of the manuscript.

Conflict of interest: Authors state no conflict of interest.

References

[1] Bąkowska A, Dobak P, Gawriuczenkow I, Kiełbasiński K, Szczepański T, Trzciński J, et al. Stress-strain behaviour analysis of Middle Polish glacial tills from Warsaw (Poland) based on the interpretation of advanced field andlaboratory tests. Acta Geol Pol. 2016;66(3):561–85. doi: 10.1515/agp-2016-0026.

[2] Kaczyński R. Warunki geologiczno-inżynierskie na obszarze Polski (Engineering-geological conditions in the area of Polish). Warszawa: PIG-PIB; 2017 (In Polish).

[3] Bogusz W, Witowski M. Preliminary assessment of variability of selected Hardening Soil model parameters for glacial tills and clays from Poland. Proceedings: 7th International Symposium on Deformation Characteristics of Geomaterials. Glasgow, UK: E3S Web of Conferences 92; 26–28 June 2019. doi: 10.1051/e3sconf/20199215004.
[4] Komadja GC, Pradhan SP, Roul AR, Adebayo B, Habinshuti JB, Glodji LA, et al. Assessment of stability of a Himalayan road cut slope with varying degrees of weathering: a finite-element-model-based approach. Heliyon. 2020;6(11):e05297. doi: 10.1016/j.heliyon.2020.e05297.
[5] Kuhn M, Mitchell J. New perspectives on soil creep. J Geotech Eng. 1993;119(3):507–24. doi: 10.1061/(ASCE)0733-9410(1993)119:3(507).
[6] Le TM, Fatahi B, Khabbaz H. Viscous behaviour of soft clay and inducing factors. Geotech Geol Eng. 2012;30(5):1069–83. doi: 10.1007/s10706-012-9535-0.
[7] Fatahi B, Le TM, Le MQ, Khabbaz H. Soil creep effects on ground lateral deformation and pore water pressure under embankments. Geomech Geoengin. 2013;8(2):107–24. doi: 10.1080/17486025.2012.727037.
[8] Grimstad G, Haji Ashrafi MA, Degago SA, Emdal A, Nordal S. Discussion of Soil creep effects on ground lateral deformation and pore water pressure under embankment. Geomech Geoengin. 2016;11(1):86–93. doi: 10.1080/17486025.2014.985338.
[9] Kaczmarek Ł, Dobak P. Contemporary overview of soil creep phenomenon. Contemp Trends Geosci. 2017;6(1):28–40. doi: 10.1515/ctg-2017-0003.
[10] Wysokiński L. Warszawska skarpa śródmiejska (Warsaw downtown slope). Warszawa: Drukarnia Piotra Włodarskiego; 1999 (In Polish).
[11] Wysokiński L. Ekspertyza dotycząca określenia uwarunkowań realizacyjnych przy budowie tuneli szlakowych D13 tarczami zmechanizowanymi TBM pod Skarpą Warszawską podczas budowy odcinka centralnego II linii metra w Warszawie (Expertise on the determination of the implementation conditions for the construction of D13 route tunnels with TBM mechanized discs under Skarpa Warszawska during the construction of the central section of the second metro line in Warsaw). Warszawa: Metro Warszawskie Sp. z o. o.; 2013 (In Polish).
[12] Piwocki M. Ewolucja poglądów na stratygrafię utworów formacji poznańskiej na Niżu Polskim (Evolution of views on the stratigraphy of the Poznań Formation in the Polish Lowlands). Prz Geol. 2002;50(3):256–7 (In Polish).
[13] Sarnacka Z. Stratygrafia osadów czwartorzędowych Warszawy i okolic (Stratigraphy Quaternary Sediment Wars its Vicin). Warszawa: Prace PIG; 1992.(In Polish).
[14] Kaczynski R. Engineering-geological evaluation of Mio-Pliocene clays in the Warsaw area, central Poland. Acta Geol Pol. 2002;52(4):437–48.
[15] Jaros M, Szlasa M. Implementation of engineering geology 3D modeling to assess geotechnical foundations requirements of the investment executed in diaphragm wall. Prz Geol. 2014;62(10/2):584–7 (In Polish).
[16] Popielski P, Siemińska-Lewandowska A. The scope of soil investigation and selection of parameters, required for the preparation of numerical models of deep foundation – experiences and conclusions. Acta Sci Pol Archit. 2016;15(4):31–42 (In Polish).
[17] Kowalczyk S, Mieszkowski R, Pacanowski G. The stability evaluation of Warsaw slope selected pieces based on Electrical Resistivity Tomography survey (ERT). Prz Geol. 2014;62(10/2):634–40 (In Polish).
[18] Kumor MK. Impact of cyclic freezing on the change of hydraulic conductivity of organic soils applied for modernization of flood embankments. Arch Hydrotech. 1985;32:461–73 (In Polish).
[19] Kaczyński R. Engineering geological behaviour of London and Warsaw clays. Geologos. 2007;11:481–90.
[20] Kaczyński R. Overconsolidation and microstructures in Neogene clays from the Warsaw area. Geol Q. 2003;47(1):43–54.
[21] Szymański A. Determination of stress history in cohesive soil on the basis of in situ tests. Proceedings: 9th Baltic Geotechnical Conference. Tallinn, Estonia: ISSMGE; 1999.
[22] ISO 14688-1:2002 Geotechnical investigation and testing – Identification and classification of soil – Part 1: Identification and description.
[23] Kaczmarek Ł, Dobak P, Kiełbasiński K. Preliminary investigations of creep strain of Neogene clay from Warsaw in drained triaxial tests assisted by computed microtomography. Stud Geotech Mech. 2017;39(2):35–49. doi: 10.1515/sgem-2017-0014.
[24] Mirvis SE. Applications of magnetic resonance imaging and three-dimensional computed tomography in emergency medicine. Ann Emerg Med. 1989;18(12):1315–21. doi: 10.1016/S0196-0644(89)80268-9.
[25] Pires LF, Cássaro FAM, Bacchi OOS, Reichardt K. Gamma-ray computed tomography in soil science: some applications. In: Saba L, editor. Comput tomography – special applications. Rijeka: InTech; 2011. p. 293–318. doi: 10.5772/23863.
[26] ISO/TS 17892-9:2004 Geotechnical investigation and testing – Laboratory testing of soil – Part 9: Consolidated triaxial compression tests on water-saturated soils.
[27] Head KH. Manual of soil laboratory testing. Effective stress tests. Vol. 3, 2nd edn. Chichester: Wiley; 1998.
[28] Lade PV. Triaxial testing of soils. Oxford: Wiley Blackwell; 2016.
[29] Black DK, Lee KL. Saturating laboratory samples by back pressure. J Soils Mech Found Div. 1973;99(SM1):75–93.
[30] Lipiński MJ, Wdowska MK. Kryteria nasączania gruntów prekonsolidowanych metodą ciśnienia wyrównawczego (Criteria for pre-consolidated soils saturation with the back pressure method). Współpraca budowli z podłożem gruntowym. Proceedings: II Problemowa Konferencja Geotechniczna (Problem Geotechnical Conference). Białystok – Białowieża, Poland: Bialystok University of Technology; 17–18 June 2004. p. 71–81
[31] Luo Q, Chen X. Experimental research on creep characteristics of Nansha soft soil. Sci World J. 2014;5:968738. doi: 10.1155/2014/968738.
[32] Bishop AW, Henkel DJ. Meas Soil Prop Triaxial Test. 2nd edn. New York: St. Martin's Press; 1962.
[33] Lambe TW. Methods of estimating settlements. J Soil Mech Found Div. 1964;90(SM5):43–67.
[34] Gasparre A, Nishimura S, Coop MR, Jardine RJ. The influence of structure on the behaviour of London Clay. Géotechnique. 2007;57(1):19–31. doi: 10.1680/geot.2007.57.1.19.

[35] Stefaniuk D, Tankiewicz M, Stróżyk J. X-ray microtomography (μCT) as a useful tool for visualization and interpretation of shear strength test results. Stud Geotech Mech. 2014;36(4):47–55. doi: 10.2478/sgem-2014-0035.
[36] Vermeer PA, Neher HP. A soft soil model that accounts for creep. Proceedings: International Symposium Beyond 2000 in Computational Geotechnics. Plaxis, Amsterdam, Netherlands: Balkema; 18–20 March 1999. doi: 10.1201/9781315138206-24.
[37] Kamoun J, Bouassida M. Creep behavior of unsaturated cohesive soils subjected to various stress levels. Arab J Geosci. 2018;11(4):1–17. doi: 10.1007/s12517-018-3399-4.
[38] Singh A, Mitchell JK. General stress–strain time function for soils. J Soil Mech Found Eng Div. 1968;94(1):21–46.
[39] Tavenas F, Leroueil S, La Rochelle P, Roy M. Creep behavior of an undisturbed lightly overconsolidated clay. Can Geo-tech J. 1978;15(3):402–23. doi: 10.1139/t78-037.
[40] Augustesen A, Liingaard M, Lade PV. Evaluation of time-dependent behavior of soils. Int J Geomech. 2004;4(3):137–56. doi: 10.1061/(ASCE)1532-3641(2004)4:3(137).
[41] Kumor MK. Selected geotechnical problems of expansive clays in the area of Poland. Archit Civ Eng Environ. 2008;1(4):75–92.
[42] Stróżyk J. The laboratory study of shear strength of the over-consolidated and quasi – overconsolidated fine – grained soil. IOP Conf Ser Earth Environ Sci. 2017;95:022055. doi: 10.1088/1755-1315/95/2/022055.
[43] Godlewski T, Kacprzak G, Witowski M. Practical estimation of geotechnical parameters for the diaphragm walldesign founded on Warsaw “pliocene” clays. Civ Environ Eng. 2013;4(1):13–9.
[44] Le T, Airey D, Standing J. Creep behaviour of undisturbed London Clay in triaxial stress space. E3S Web Conf. 2019;92(05006):1–6. doi: 10.1051/e3sconf/20199205006.
[45] Zimmermann Th, Rodriguez C, Dendrou B. Z_SOIL.PC: A program for solving soil mechanics problems on a personal computer using plasticity theory. Proceedings: Conference on Geomechanics. Innsbruck, Austria: Balkema; 11–15 April 1988.
[46] Zabuski L, Świdziński W, Kulczykowski M, Mrozek T, Laskowicz I. Monitoring of landslides in the Brda river valley in Koronowo (Polish Lowlands). Env Earth Sci. 2015;73:8609–19. doi: 10.1007/s12665-015-4025-3.
[47] Hight DW, Gasparre A, Nishimura S, Minh NA, Jardine RJ, Coop MR. Characteristics of the London Clay from the Terminal 5 site at Heathrow airport. Géotechnique. 2007;57(1):3–18. doi: 10.1680/geot.2007.57.1.3.
[48] Dadlez R, Jaroszewski W. Tektonika (Tectonics). Warszawa: Wyd. PWN; 1994 (In Polish).